Journal of Cardiology 73 (2019) 438–444

Contents lists available at ScienceDirect

Journal of Cardiology

journal homepage: www.elsevier.com/locate/jjcc

Original article

Novel phenotype–genotype correlations of hypertrophic cardiomyopathy caused by mutation in α-actin and myosin-binding protein genes in three unrelated Chinese families

Qian-Li Yang (MS)[a,†], Yang-Yang Bian (MD)[b,†], Bo Wang (MS)[a], Lei Zuo (MD)[a], Meng-Yao Zhou (MS)[a], Hong Shao (MD)[c], Yan-Min Zhang (MD)[d,**], Li-Wen Liu (MD)[a,*]

[a] Department of Ultrasound, Xijing Hospital, Fourth Military Medical University, Xi'an, Shaanxi, China
[b] Medical Research Centre, The First Affiliated Hospital of Zhengzhou University, Henan, Zhengzhou, China
[c] Department of Cardiology, Xijing Hospital, Fourth Military Medical University, Xi'an, Shaanxi, China
[d] Children's Research Institute, Department of Cardiology, Affiliate Children's Hospital of Xi'an Jiaotong University, Xi'an, Shannxi, China

ARTICLE INFO

Article history:
Received 14 June 2018
Received in revised form 3 September 2018
Accepted 24 September 2018
Available online 29 December 2018

Keywords:
Hypertrophic cardiomyopathy
ACTC1-D26N and *MYBPC3*-R215C
Genotype and phenotype
Triphasic left ventricular filling pattern

ABSTRACT

Background: The correlations between genotype and phenotype in hypertrophic cardiomyopathy (HCM) have not been established. Mutation of α-actin gene (*ACTC1*) is a rare cause of HCM. This study aimed to explore novel genotype–phenotype correlations in HCM patients with the variants in *ACTC1* and myosin-binding protein (*MYBPC3*) genes in three unrelated Chinese families.

Methods: Clinical, electrocardiographic, and echocardiographic examinations were performed in three Han pedigrees. Exon and boarding intron analysis of 96 cardio-disease-related genes was performed using second-generation sequencing on three probands. The candidate variants were validated in 14 available family members and 300 unrelated healthy controls by bi-directional Sanger sequencing. The pathogenicity and conservation were calculated using MutationTaster, PolyPhen-2, SIFT, and Clustal X. Pathogenicity classification of the variants was based on American College of Medical Genetics and Genomics (ACMG) guidelines.

Results: Nine members fulfilled diagnostic criteria for HCM with clinical characteristics, electrocardiographic, and echocardiographic findings. Two candidate variants in *ACTC1* p.Asp26Asn (*ACTC1*-D26N) and *MYBPC3* p.Arg215Cys (*MYBPC3*-R215C) were identified in patients. Only *ACTC1*-D26N strongly co-segregated with the HCM phenotype. Seven patients who harbored variant *ACTC*-D26N only were diagnosed with non-obstructive HCM, and four of these patients exhibited a triphasic left ventricular (LV) filling pattern. Two patients carrying both *ACTC1*-D26N and *MYBPC3*-R215C variants showed a higher LV outflow tract pressure gradient. Bioinformatics analysis revealed that the two variants were deleterious and highly conserved across species. According to ACMG guidelines, *ACTC1*-D26N is classified as a likely pathogenic mutation. The second variation *MYBPC3*-R215C may function as a genetic modifier, which remains uncertain here.

Conclusions: Novel p.(Asp26Asn) mutation of ACTC1 was associated with HCM phenotype, and the penetrance is extremely high (~81.8%) in adults. The second variation, *MYBPC3*-R215C may function as a genetic modifier, which remains uncertain here.

Introduction

Hypertrophic cardiomyopathy (HCM) is a common inherited cardiac disease with an estimated prevalence of 1 in 200 [1]. It is the main cause of sudden death (SD) in young people and athletes (≈1% per year) [2]. To date, more than 1500 variations in genes encoding cardiac sarcomere proteins have been identified in HCM patients [3]. Most genotyped of HCM patients have revealed

* Corresponding author at: Department of Ultrasound, Xijing Hospital, Fourth Military Medical University, 127# Changle West Road, Xi'an, Shaanxi, China.
** Corresponding author at: Children's Research Institute, Department of Cardiology, Affiliate Children's Hospital of Xi'an Jiaotong University, No. 69, Xijuyuan Land, Xi'an, Shannxi, China.
†Corresponding authors.
E-mail addresses: ymzh628@126.com (Y.-M. Zhang), liuliwen@fmmu.edu.cn (L.-W. Liu).

https://doi.org/10.1016/j.jjcc.2018.09.005
0914-5087/

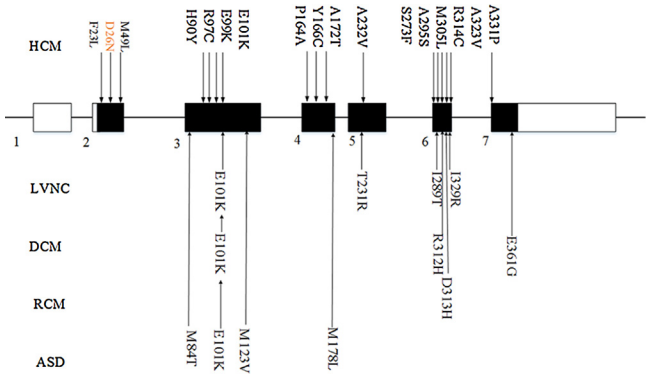

Fig. 1. Structure of the *ACTC1* indicating the positions of the variants. Previously reported in the literature (black) and our data (orange). ASD, atrial septal defect; DCM, dilated cardiomyopathy; HCM, hypertrophic cardiomyopathy; LVNC, left ventricular noncompaction cardiomyopathy; RCM, restrictive cardiomyopathy.

defects in thick-filament genes. However, for a small proportion of HCM patients, the disease is caused by mutations in thin-filament genes [4,5]. For such patients, there is limited understanding of clinical presentation and outcomes.

The cardiac α actin gene (*ACTC1*) is the main component of thin-filament genes in mature cardiac myocytes and is completely conserved across species from avians to mammals. It is critical for normal cardiac morphogenesis and muscle contraction [6]. Mutations in *ACTC1* have been phenotypically related to various cardiac anomalies including dilated cardiomyopathy (DCM), restrictive cardiomyopathy (RCM), left ventricular non-compaction (LVNC), HCM, and congenital heart disease (CHD) [7–9]. Fig. 1 shows all 26 mutations in the *ACTC1* gene reported in the literature [8–18]. Mutations in *ACTC1* appear to be a rare cause of HCM (<1%) [5], and only 15 mutations linked to HCM have been reported to date.

It is well-established that ~1.7% of HCM patients harbor ≧2 variants in sarcomere protein genes. Compared to patients with a single mutation, these patients seem to have a more severe HCM phenotype [19]. Up to 30% of mutations in HCM were detected in the myosin-binding protein C (*MYBPC3*) gene, which encodes the thick-filament protein. Mutations in *MYBPC3* seem to be associated with late-onset hypertrophy and a favorable clinical course [20]. The clinical presentation of HCM is highly heterogeneous, including disease severity, age of onset, and disease progression. It is difficult to predict disease severity because of variable penetrance and insufficient genotype–phenotype correlation [21].

Therefore, we conducted this study to analyze the correlations between variants of *ACTC1*-D26N and *MYBPC3*-R215C and their correlations with HCM phenotypes in three Chinese families.

Materials and methods

Subjects and clinical evaluation

This study was conducted in accordance with the principles of the Declaration of Helsinki and approved by the ethics committee of Xijing Hospital, Fourth Military Medical University, PRC. This study includes 14 members (five males and nine females) from three unrelated Chinese Han families, with clinical data of medical history, 12-lead electrocardiograms (ECG), and echocardiograms (UCG).

Diagnostic criteria for HCM and UCG examination

According to the 2014 European Society of Cardiology Guidelines on Diagnosis and Management of Hypertrophic Cardiomyopathy [22], HCM in adults is recognized by a maximal left ventricular wall thickness (MLVWT) ≧15 mm in one or more LV myocardial segments or ≧13 mm in first-degree relatives of the patients that is not explained solely by loading conditions. For children, a diagnosis of HCM requires a wall thickness ≧2 SD above the predicted mean (z score ≧ 2) for age, sex, or body size.

UCG was carried out using the Philips iE33 ultrasound system (Philips Medical Systems, Bothell, WA, USA) with a multi-frequency matrix probe. Patients were placed in the left lateral decubitus position, and ECG was recorded simultaneously. MLVWT, LV ejection fraction, left atrial (LA) diameter, and LV outflow tract pressure gradient (LVOT-PG) were estimated in accordance with the guidelines of the American Society of Echocardiography [23]. LV filling patterns were assessed by pulsed-wave Doppler at the mitral tip level and tissue Doppler at the lateral mitral annulus velocity. A triphasic LV filling pattern was considered present when a velocity peak of at least 0.2 m/s (L-wave) was observed during diastasis independent of overall LV filling pattern [24,25].

Genetic analysis and bioinformatics prediction

Genomic DNA was isolated from 4 mL of peripheral blood using a DNA Maxi Kit (D2492, Omega Bio-Tek, Inc., Norcross, GA, USA) following the standard protocols. The target panel included 96 cardio-disease-related genes; the gene list is shown in Table 1. The enriched libraries were sequenced using an SolexaHiSeq 2000 sequencer (Illumina, San Diego, CA, USA) by targeted exome capture. Low-quality reads and adaptor sequences were filtered out. A high-quality sequencing depth (380.29) was mapped for targeted regions, which accounted for approximately ~99.7% on 96 genes. After annotation of the identified single nucleotide polymorphisms and InDels (insertions or deletions), the candidate variants were validated in available family members and 300 unrelated healthy controls by bi-directional Sanger sequencing.

The pathogenicity of candidate variants was calculated using Sorting Intolerant From Tolerant (SIFT, http://sift.jcvi.org), Polymorphism Phenotyping v2 (PolyPhen-2, http://genetics.bwh.harvard.edu/pph2/), and MutationTaster (http://www.mutationtaster.org). The conservation of candidate variants was evaluated using Cluster X (http://www.clustal.org/clustal2/) in multiple species (including *Homo sapiens*, *Pan paniscus*, *Sus scrofa*, *Bos taurus*, *Rattus norvegicus*, *Mus musculus*, *Papio anubis*, *Lonchura striata domestica*, *Xenopus laevis*, and *Danio rerio*).

Prediction of the structure of the protein encoded by the ACTC1-D26N mutation

The three-dimensional (3D) structure of the protein encoded by *ACTC1*-D26N was analyzed using the Rigor Actin-Tropomyosin-Myosin complex (ATM) (PDB accession codes 4A7F, https://www.rcsb.org/structure/4A7F) and the SWISS-MODEL (http://swissmodel.expasy.org/) [26]. Residues for interaction between myosin and specific actin were further analyzed. Images were prepared using the PyMOL molecular graphics system (PyMOL, https://pymol.org/2/).

Pathogenicity classification

The candidate variants were evaluated by the variant-classification guidelines of the American College of Medical Genetics and Genomics (ACMG) guidelines [27]. First, we searched for information in population databases [Exome Aggregation Consortium, Exome Variant Server (EVS)], disease databases (ClinVar, OMIM, Human Gene Mutation Database), and the scientific literature for assessment of the clinical significance. Second, computational predictions for *ACTC1*-D26N were calculated by SIFT, PolyPhen-2,

Table 1
The list of 96 cardiac-related genes screened in this study.

AARS2, ABCC1, ABCC9, ACTC1, ACTN2, AKAP9, ANK2, ANKRD1, BAG3, BRAF, CACNA1C, CACNB2, CASQ2, CAV3, CBL, CRYAB, CSRP3, DES, DMD, DSC2,DSG2, DSG3, DSP, DTNA, EMD, EYA4, FHL2, FHOD3, FKTN, GATAD1, GLA, GPD1L, HCN4, ILK, JPH2, JUP, KCNE1, KCNE2,KCNE3, KCNH2, KCNJ2, KCNJ5,KCNQ1, KRAS, LAMP2, LDB3, LMNA, MARCKSL1, MYBPC3, MYH6, MYH7, MYL2, MYL3, MYLK2, MYOZ2, MYPN, NEXN, NRAS, OBSCN, PDLIM3, PKP2, PLB1,PLN, PRKAG2, PSEN1, PSEN2, PTPN11, RAF1, RBM20, RYR2, SCN1B, SCN3B, SCN4B, SCN5A, SCO2, SGCD, SHOC2, SLC25A4, SNTA1, SOS1, TAZ, TCAP,TGFB3, TMEM43, TMEM70, TMPO, TNNC1, TNNC2, TNNI3, TNNT2, TNNT3, TPM1, TRPC6, TTN, TTR, VCL

Table 3
Results of mutation prediction algorithms for two candidate variants detected in this study.

Algorithm	PolyPhen-2		Mutation Taster		SIFT	
Variant	*ACTC1* -D26N	*MYBPC3* -R215C	*ACTC1* -D26N	*MYBPC3* -R215C	*ACTC1* -D26N	*MYBPC3* -R215C
Score	0.88	0.983	23	180	0.01	0.02
Prediction	Possibly damaging		Disease causing		Affect protein function	

MutationTaster and Cluster X (Cluster X, http://www.clustal.org/clustal2/). Third, familial segregation analysis was performed, wherever possible, using a recently described method for consideration of co-segregation of a variant and a disease in the classification of variant pathogenicity [28].

Results

Clinical and phenotypic characteristics

A total of 14 family members (five males and nine females), including the proband of each family, were clinically examined. Fig. 2 shows the pedigrees of families (Family F1, F2, and F3). Nine members met the echocardiogram diagnostic criteria for HCM. The results of the clinical characteristics and genetic testing of the pedigrees are summarized in Table 2.

The symptomatic presentation of the patients was diverse. Two patients (F1-I1 and F3-II2) complained of syncope, fatigue, and angina. Four patients (F1-II1, F2-II3, F3-III1, and F3-III2) experienced chest tightness, palpitation, and dyspnea on exertion. Three patients (F2-I1, F3-II5, and F3-II7) had no relevant clinical symptoms after physical activity. A maternal aunt of F2-II3 died suddenly at age 46 years. F3-II2 had a pacemaker implanted due to sick sinus syndrome when she was 64 years. F3-III1 had received surgery for patent ductus arteriosus.

The ECG results revealed repolarization abnormalities including ST segment depression or elevation, T wave flatness or inversion, or left ventricular hypertrophy with strain. Three patients (F3-II2, F3-II5, and F3-II7) had experienced atrial fibrillation. The UCG results showed increased LV wall thickness with MLVWT ranging from 15 to 29 mm and involvement of the interventricular septum (the basal anterior interventricular septum or the midventricular anterior interventricular septum). Eight patients were diagnosed with non-obstructive hypertrophic cardiomyopathy (non-obstructive HCM). Only F2-I1 was diagnosed with obstructive hypertrophic cardiomyopathy (LVOT-PG: 33 mmHg). Except for F2-II3, all patients showed LA enlargement (41–88 mm). All patients had diastolic abnormalities, and four patients (F1-I1, F1-II1, F3-III1, and F3-III2) exhibited a triphasic LV filling pattern with heart rates in the range of 49–61 beats per minute (bpm). Patients F3-III4 had been diagnosed with HCM at 20 years and presented with a normal ECG at other hospitals. Five members (F1-I2, F2-II1, F3-II3, F3-III5, and F3-III6) had a normal phenotype.

Genetic analysis and bioinformatics prediction

Two variants of *ACTC1*-D26N (c.76G>A, Asp26Asn) and *MYBPC3*-R215C (c.643C>T, Arg215Cys) were detected in the families (Sanger sequencing analysis shown in Fig. 3A). F1-I2 and F3-II3 harbored neither of the two variants. Except for F2-II1, all other members harbored variants of *ACTC1*-D26N: F2-I1 and F2-II3 carried two variants of *ACTC1*-D26N and *MYBPC3*-R215C, whereas F2-II1 harbored only a variant of *MYBPC3*-R215C.

The two variants were absent in the 300 healthy controls. They are reported as variants of uncertain significance in ClinVar, a public archive of reports of clinical significance of variants (https://www.ncbi.nlm.nih.gov/clinvar/). There is only one study reporting *MYBPC3*-R215C in a HCM patient in the Chinese population [11]. There are no detailed clinical descriptions of patients harboring variants *ACTC1*-D26N or *MYBPC3*-R215C.

ACTC1-D26N (c.76G>A, Asp26Asn) represented c.76G>A within exon 2 of *ACTC1*, resulting in a negatively charged aspartate residue

Table 2
The results of the clinical characteristics and genetic testing of the pedigrees.

Case	Sex/Dx (y)	Years	Genotype	Phenotype	ECG parameter			Echocardiography parameter			
					Heart rate	ST-T change	LVH	MLVWT (mm)	LVOT-PG (mmHg)	LA (mm)	L wave
F1-I 1	F/40	45	A	HCM	54	Y	N	22	3	48	Y
F1-I 2	M/–	46	–	Normal	73	N	N	10	5	32	N
F1-II 1	M/17	19	A	HCM	49	Y	Y	19	5	41	Y
F2-I 1	F/64	64	A, B	HCM	89	Y	Y	26	33	41	N
F2-II 1	M/–	39	B	Normal	69	N	N	10	3	24	N
F2-II 3	M/32	37	A, B	HCM	67	Y	N	19	12	36	N
F3-II 2	F/19	63	A	HCM	52	Y	N	15	5	44	N
F3-II 3	F/–	58	–	Normal	73	N	N	12	8	40	N
F3-II 5	F/18	53	A	HCM	AF	Y	Y	22	15	56	N
F3-II 7	F/40	47	A	HCM	AF	Y	N	24	2	88	N
F3-III 1	F/33	37	A	HCM	61	Y	N	16.8	3	44	Y
F3-III 2	F/33	33	A	HCM	55	Y	Y	29	2	44	Y
F3-III 5	F/–	10	A	Normal	87	N	N	8.3	4	26	N
F3-III 6	M/–	8	A	Normal	84	N	N	9.8	3	29	N

Dx (y), age at diagnosis the age of onset of HCM was defined as the first diagnosis according to hospital records; years, age at clinical evaluation; A, *ACTC1*-D26N; B, *MYBPC3*-R215C.
ECG, electrocardiogram; ST-T change, ST-segment depression or elevation, T wave flatness or inversion; LVH, left ventricular high voltage; MLVWT (mm), maximum left ventricular wall thickness; LVOT-PG (mmHg), LV outflow tract pressure gradient; LA(mm), left atrial diameter; L wave, prominent mid-diastolic flow velocity when a velocity peak of at least 0.2 m/s; HCM, hypertrophic cardiomyopathy; N/A, not applicable; AF, atrial fibrillation.

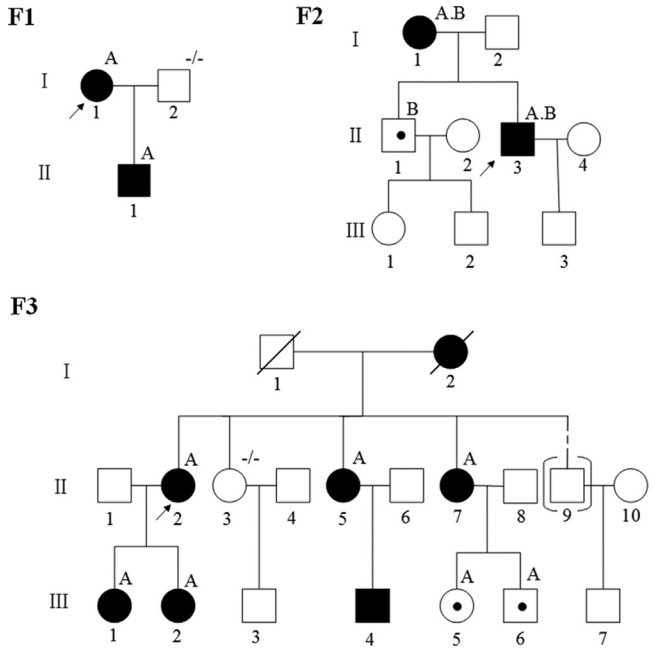

Fig. 2. Pedigrees of family F1, F2, and F3 with phenotypic and genotypic information. I, II, and III refer to the first, second, and third generations of each family. Square symbols represent males, circle symbols denote females. Filled black symbols represent patients with hypertrophic cardiomyopathy, symbols with dots represent mutation carriers without clinical manifestation. White symbols denote unavailable family members. The arrows indicate the proband of each family. The genotype for each individual noted above the symbol where available. (A) *ACTC1*-D26N; (B) *MYBPC3*-R215C.

(Asp, D) to a neutral asparagine (Asn, N) at position 26, located within a negatively charged loop from actin SD1 in the ACTC1 protein. *MYBPC3*-R215C represented one base transformation in codon 215 (c.643C>T) in exon 5 of *MYBPC3*, resulting in a change from arginine (Arg, R) to cysteine (Cys, C), located within the C1 domain of the MYBPC3 protein. It is reported that the C0–C4 domains of cMyBP-C extend into the interfilament space, where they could interact with myosin-S2 and actin [29].

The pathogenicity of the two variants was predicted to be damaging using multiple software programs (details shown in Table 3). Sequence alignment showed that the residues of Asp26 in ACTC1 and Arg215 in MYBPC3 are highly conserved in diverse species (Fig. 3B).

Genotype–phenotype correlations

To determine genotype–phenotype relationships and the pathogenesis of variants identified in this study, the results of genetic testing, clinical features, ECG results, and UCG results were further analyzed.

ACTC1-D26N was shared by nine patients. Seven of them (F1-I1, F1-II1, F3-II2, F3-II5, F3-II7, F3-III1, and F3-III2) only harbored *ACTC1*-D26N. The other two patients (F2-I1 and F2-II3) carried both *ACTC1*-D26N and *MYBPC3*-R215C.

Seven patients harboring *ACTC1*-D26N only were diagnosed with non-obstructive HCM (LVOT-PG <30 mmHg at rest). Patients may have mild or moderate LV hypertrophy (Fig. 4A and B, F3-III1 and F3-III2 with maximal wall thickness of 16.8 mm, 29 mm, respectively). LA dilation was common in patients, with F3-II7 showing remarkable LA dilation and her ECG revealing atrial fibrillation (Fig. 4C and D). Patients also showed diastolic abnormalities: four patients exhibited a triphasic LV filling pattern (Fig. 4E) with a heart rate in the range of 52–61 bpm. Compared with patients who carried mutation *ACTC1*-D26N only, F2-I1 and F2-II3 showed higher LVOT-PG (Fig. 4F, patient F2-I1, LVOT-PG: 33 mmHg). They also showed diastolic dysfunction, but a triphasic LV filling pattern was not observed. A maternal aunt of F2-II3 died suddenly, although HCM could not be verified as the cause of death. F3-III5 and F3-III6, who harbored variant *ACTC1*-D26N, require re-evaluation because they were only 10-years-old and 8-years-old, respectively, at the last evaluation. F2-II1 with variant *MYBPC3*-R215C had a normal phenotype at age 39 years. F1-I2 and F3-II3 showed a normal phenotype who harbored neither of the two variants mentioned above.

Our observations indicate that *ACTC1*-D26N co-segregated strongly with HCM phenotype in adults within families. Thus, *ACTC1*-D26N could be a major gene, whereas *MYBPC3*-R215C may function as a genetic modifier, which remains uncertain here.

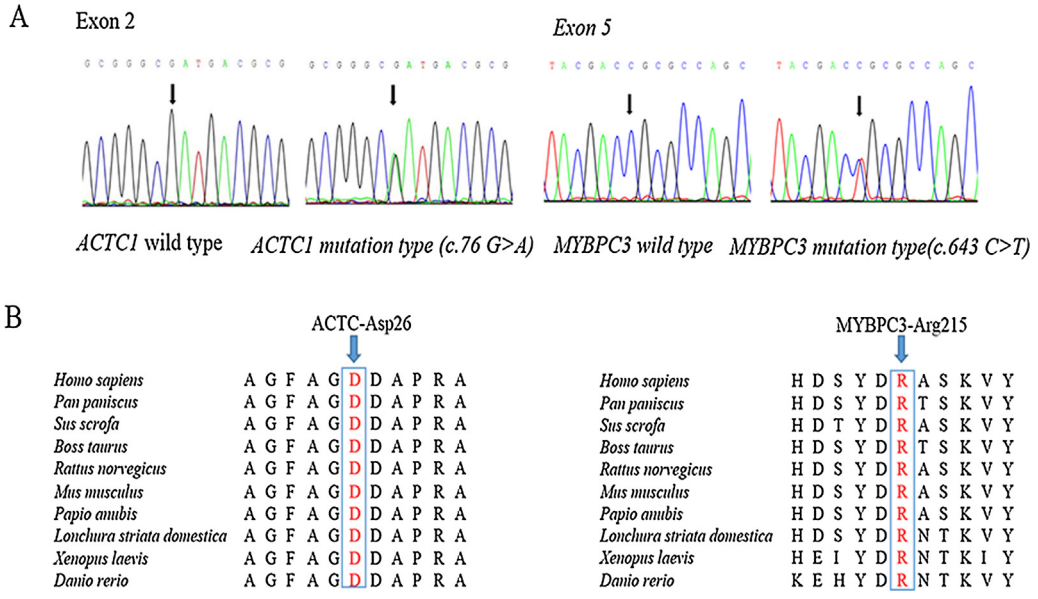

Fig. 3. Mutation screening and conservative analysis. (A) DNA sequences of wild-type (left) and mutant (right) were validated by Sanger sequencing. (B) Alignment of this region of *ACTC1* amino acid sequence from multiple species demonstrating the conservation of the position 26 (black arrow index).

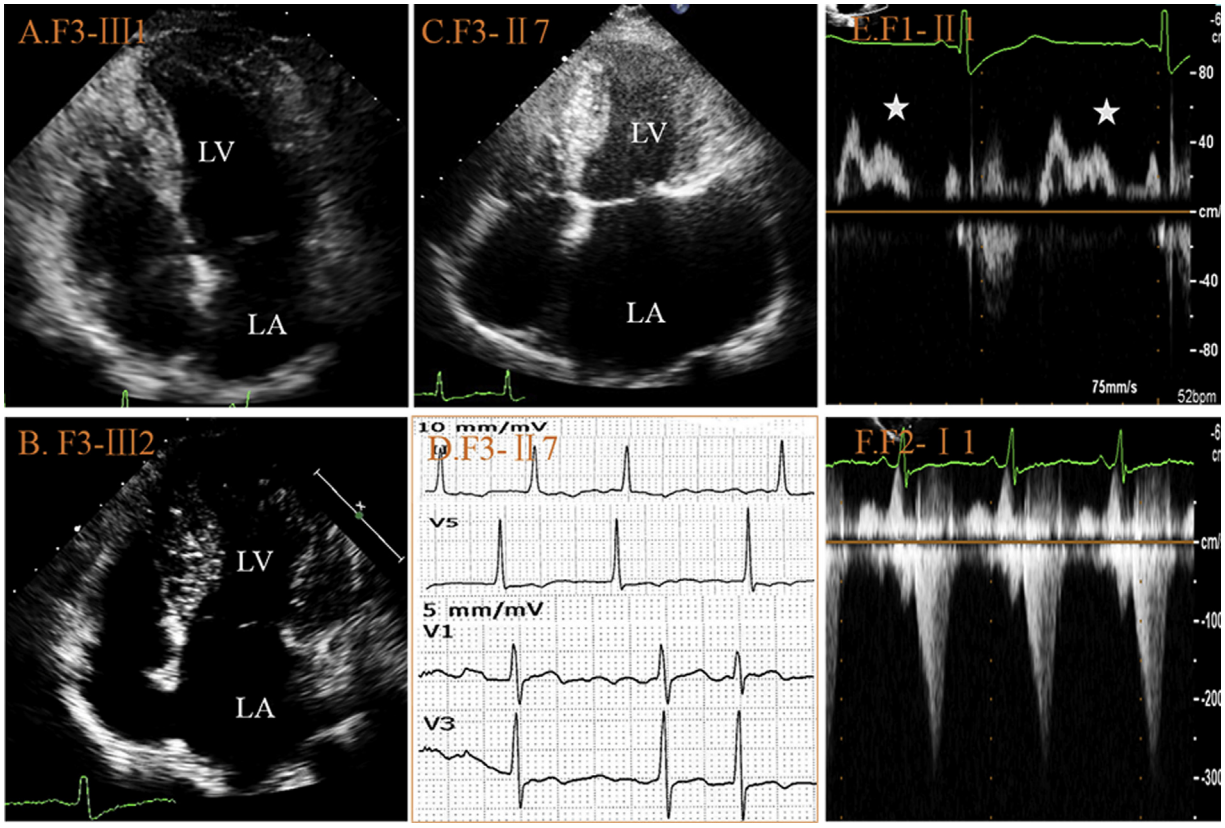

Fig. 4. (A) Mild hypertrophy associated with *ACTC1*-D26N (patient F3-III1). (B) Moderate hypertrophy associated with *ACTC1*-D26N (patient F3-III2). (C) Moderate hypertrophy and marked left atrial dilation associated with *ACTC1*-D26N (patient F3-II7). (D) Electrocardiogram showed atrial fibrillation (patient F3-II7). (E) Representative transmitral blood flow velocity patterns assessed by pulsed-wave Doppler echocardiography, mid-diastolic flow velocity (L-wave) is clearly visible (asterisk index) (patient F1-II1) (F) Left ventricular outflow tract, 33 mmHg, F2-II2 harboring mutations *ACTC1*-D26N and *MYBPC3*-R215C. LA, left atrium; LV, left ventricle.

Bioinformatics analysis and mutation protein structure prediction

3D structure analysis showed that p.D26 is exposed on the surface region of F-actin (Fig. 5A) and is involved in the formation of a negatively charged loop from actin SD1 (residues 20–28 [D24, D25]) (Fig. 5B and C). Actin SD1 can make contact with conserved positively charged residues within the myoE CM loop (R323, K331, R332) and helix HX (K556, K557, R558, R567) by the formation of salt bridges [26]. Thus, changes in the charge of position 24 of ACTC1 may disrupt interactions between actin and myosin. Note that the first two residues are removed during actin maturation, and D26N should be described as D24N. Salt bridges are the most common non-covalent interactions that help to stabilize the conformation of proteins. Residue R332 corresponded to human β-cardiac myosin R403, which is associated with a severe form of HCM.

Classification of the variations

Data mining of public population cohorts, variant databases, and the scientific literature indicated that only *ACTC1*-D26N is included in ClinVar and that its clinical significance is uncertain. This variant was encoded as PM2 based on ACMG. Computational predictions supported a deleterious effect, and the position of p. D26 was highly conserved across species and it was encoded as PP3. Segregation analysis of HCM phenotype with genotype (*ACTC1*-D26N) was perfect. According to a method mentioned above, the evidence level of pathogenicity can be encoded as PP1-Strong ($N \leq 1/16$ in three families).

Variant *ACTC1*-D26N met the following criteria: PP1-Strong; PM2; PP2; PP3; PP4, and can thus be classified as a likely pathogenic mutation according to ACMG guidelines. Because of insufficient evidence, *MYBPC3*-R215C is still classified as a variant of uncertain significance.

Discussion

The present study identified two heterozygous mutations of *ACTC1*-D26N and *MYBPC3*-R215C in three families. *ACTC1*-D26N was identified as a likely diseasing-causing mutation in this study. The second variation *MYBPC3*-R215C may function as a genetic modifier, which remains uncertain here because the family was small and screening for other relatives was unavailable. *ACTC1* encodes cardiac muscle alpha actin, which is critical for maintaining normal structure and generating contractions of the heart. Mice lacking ACTC1 do not survive more than two weeks, and knockdown of ACTC1 in chick embryos causes ASD [8,30]. The conserved nature implies that a change in any residue will affect basic functions, including polymerization, interaction with *Z* lines, binding with regulatory proteins, or interactions with myosin or other sarcomere proteins [31,32]. Mutant actin can be integrated into cardiomyocyte thin filaments. Function analysis of variants p. M123V and p.E99K demonstrated reduced affinity for myosin compared with the wild type, and p.E99K had slower motility, reduced average force, and weakened interactions with myosin in the presence of ATP [10,16]. The variants p.Y166C and p.M305L display disturbed intrinsic ATPase activity, with the p.Y166C mutant showing a reduced rate (about 20-fold reduced), and the p. M305L mutant showing an increased rate (3.5-fold increased) as well as altered polymerization behavior [33]. Mutation p.F169S causes severe inherent filament destabilization, leading to disassembly of F-actin into small annealing incompetent filament

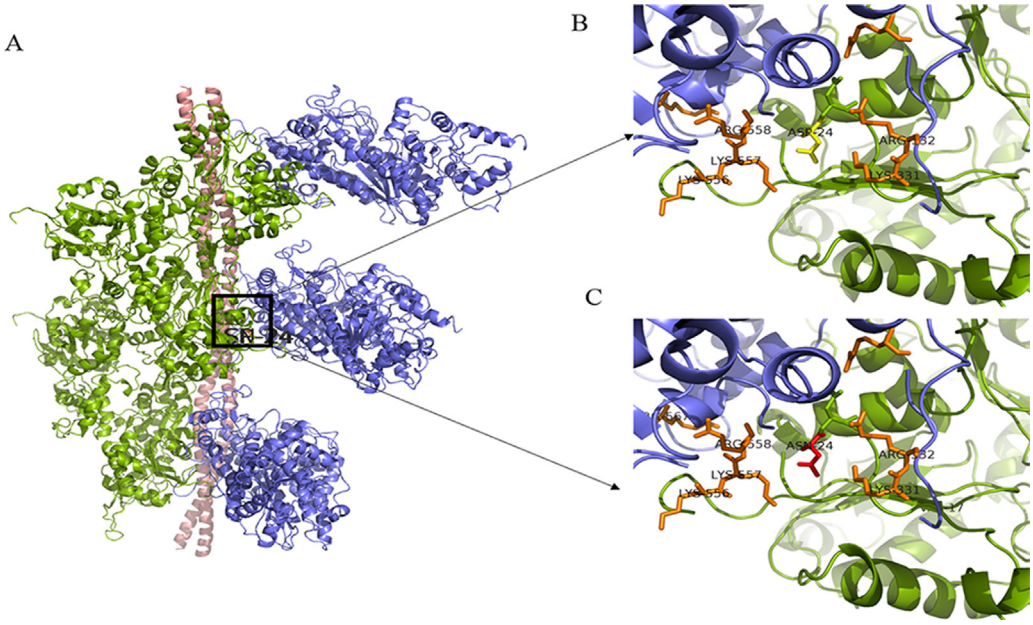

Fig. 5. (A) Predict structure of *ACTC1*-D26N-tropomyosin-myosin complex by analyzing the rigor actin-tropomyosin-myosin complex (PDB accession codes 4A7F, https://www.rcsb.org/structure/4A7F) actin fiber (split pea green), myosin heads (slate blue), tropomyosin (salmon red). (B)Wild type, close up on the interaction between the negatively charged residue D24 of F-actin monomer and positively charged residues on the myo-IE CM loop (R323, K331, R332) and helix HX (K556, K557, R558, R567), these charged residues were shown in sticks, D24 is colored yellow, the others are colored orange. (C) Mutation type, close up on the interaction between residue N24 of F-actin monomer and myo-IE CM loop (R323, K331, R332) and helix HX (K556, K557, R558, R567), these charged residues are shown in sticks, N24 is colored red, the others are colored orange.

fragments [34]. Mutation p.A331P significantly decreases the contractility and Ca^{2+} sensitivity of the reconstituted fibers [31]. Such changes at the molecular level appear to be the basis for the initiation of the discordant phenotypes seen in cardiomyopathies.

A genotype–phenotype correlation was determined in our work. Family members with mutation *ACTC1*-D26N developed HCM in adulthood. The phenotype of patients carrying only the variant *ACTC1*-D26N was distinct from thick-filament HCM patients. Nearly all cases were of non-obstructive HCM. The maximal LV thickness site is exhibited in interventricular septum hypertrophy, and it is not difficult to find differences in MLVWTs. Diastolic abnormalities are common in HCM patients. It is worth mentioning that a triphasic LV filling pattern was observed in four patients with *ACTC1*-D26N. The presence of an L-wave has been associated with advanced diastolic impairment, slow heart rate, extensive septal fibrosis, and worse prognosis [35–37]. An L-wave is independent of the overall diastolic pattern, with E/A ratios that can be <1 (i.e. delayed relaxation) or >1 (i.e. pseudo normalized). It is reported that only 11% of thick-filament patients and 26% of thin-filament patients exhibited a triphasic LV filling pattern [38]. Although they had mild or even no symptoms, LA remodeling was detected in our patients.

The penetrance of *ACTC1*-D26N is extremely high ($\sim$81.8%). It is well-known that the penetrance of the HCM phenotype is age-related, and appearance of the phenotype is often delayed until adulthood. Further follow-up is required to verify whether two carriers in our study, F3-III 5 and F3-III 6, are HCM patients. The clinical and genetic data for F3-III 4 that we could not obtain affected the calculation of penetrance of *ACTC1*-D26N.

MYBPC3 encodes the cardiac myosin-binding protein C (MYBPC3), which is arrayed in sarcomere A-bands and binds MYH7 in thick filaments and TTN in elastic filaments. In patients with HCM, up to 30% of mutations are detected in MYBPC3. In our study, two patients (F2-I1 and F2-II3) with both *MYBPC3*-R215C and *ACTC1*-D26N mutations exhibited higher LVOT-PG and diastolic dysfunction, but an L-wave was not detected. F2-II1 only carried *MYBPC3*-R215C and had a normal phenotype. It has been extensively reported that the presence of two (or even three) sarcomere mutations in an individual patient promotes greater disease severity and may influence the natural history [39]. Obvious cumulative effects have not been found, as the phenotype of *MYBPC3* mutation is associated with mild hypertrophy, late-onset, incomplete penetrance, and better prognosis [40]. It is possible that *MYBPC3*-R215C may affect the degree of HCM severity.

Limitations

There are several limitations to our study. First, the number of HCM patients was limited and the obtained clinical data were not consistent for all subjects, which affected the calculation of penetrance of *ACTC1*-D26N. Second, no functional experiments were performed and the pathogenic mechanisms of *ACTC1*-D26N remain speculative. Third, no cardiovascular events were observed. In our future work, we aim to continue recruiting HCM patients with a family history of HCM and perform long-term follow-up.

Conclusion

In this study, nine of eleven members with *ACTC1*-D26N had HCM. Disease penetrance among mutation carriers was 81.8% for subjects older than 16 years with MLVWT $\geq$15 mm. It should be noted that *ACTC1*-D26N appears to be associated with relatively low morbidity, high penetrance, and diverse phenotypes. The second variation, *MYBPC3*-R215C may function as a genetic modifier, which remains uncertain here.

Funding

This article was supported by International Cooperation Funding of the China Science and Technology Ministry (2014DFA31980), National Natural Science Foundation of China (81671693, 30371571, 81470452), and Shaanxi Provincial Key Project (2017ZDXM-SF-058).

Conflict of interest

The authors declare that there is no conflict of interest.

References

[1] Semsarian C, Ingles J, Maron MS, Maron BJ. New perspectives on the prevalence of hypertrophic cardiomyopathy. J Am Coll Cardiol 2015;65:1249–54.
[2] Maron BJ, Olivotto I, Spirito P, Casey SA, Bellone P, Gohman TE, et al. Epidemiology of hypertrophic cardiomyopathy-related death: revisited in a large non-referral-based patient population. Circulation 2000;102:858–64.
[3] Maron BJ, Ommen SR, Semsarian C, Spirito P, Olivotto I, Maron MS. Hypertrophic cardiomyopathy: present and future, with translation into contemporary cardiovascular medicine. J Am Coll Cardiol 2014;64:83–99.
[4] McNally EM, Barefield DY, Puckelwartz MJ. The genetic landscape of cardiomyopathy and its role in heart failure. Cell Metab 2015;21:174–82.
[5] Veselka J, Anavekar NS, Charron P. Hypertrophic obstructive cardiomyopathy. Lancet 2017;389:1253–67.
[6] Vandekerckhove J, Bugaisky G, Buckingham M. Simultaneous expression of skeletal muscle and heart actin proteins in various striated muscle tissues and cells. A quantitative determination of the two actin isoforms. J Biol Chem 1986;261:1838–43.
[7] Mogensen J, Perrot A, Andersen PS, Havndrup O, Klausen IC, Christiansen M, et al. Clinical and genetic characteristics of alpha cardiac actin gene mutations in hypertrophic cardiomyopathy. J Med Genet 2004;41:e10.
[8] Matsson H, Eason J, Bookwalter CS, Klar J, Gustavsson P, Sunnegardh J, et al. Alpha-cardiac actin mutations produce atrial septal defects. Hum Mol Genet 2008;17:256–65.
[9] Yoshida Y, Hirono K, Nakamura K, Suzuki T, Hata Y, Nishida N. A novel ACTC1 mutation in a young boy with left ventricular noncompaction and arrhythmias. Heart Rhythm Case Rep 2016;2:92–7.
[10] Bookwalter CS, Trybus KM. Functional consequences of a mutation in an expressed human alpha-cardiac actin at a site implicated in familial hypertrophic cardiomyopathy. J Biol Chem 2006;281:16777–84.
[11] Zou Y, Wang J, Liu X, Wang Y, Chen Y, Sun K, et al. Multiple gene mutations, not the type of mutation, are the modifier of left ventricle hypertrophy in patients with hypertrophic cardiomyopathy. Mol Biol Rep 2013;40:3969–76.
[12] Maron BJ, Maron MS, Semsarian C. Double or compound sarcomere mutations in hypertrophic cardiomyopathy: a potential link to sudden death in the absence of conventional risk factors. Heart Rhythm 2012;9:57–63.
[13] Morita H, Rehm HL, Menesses A, McDonough B, Roberts AE, Kucherlapati R, et al. Shared genetic causes of cardiac hypertrophy in children and adults. N Engl J Med 2008;358:1899–908.
[14] Olson TM, Doan TP, Kishimoto NY, Whitby FG, Ackerman MJ, Fananapazir L. Inherited and de novo mutations in the cardiac actin gene cause hypertrophic cardiomyopathy. J Mol Cell Cardiol 2000;32:1687–94.
[15] Augiere C, Megy S, El Malti R, Boland A, El Zein L, Verrier B, et al. A novel alpha cardiac actin (ACTC1) mutation mapping to a domain in close contact with myosin heavy chain leads to a variety of congenital heart defects, arrhythmia and possibly midline defects. PloS One 2015;10:e0127903.
[16] Greenway SC, McLeod R, Hume S, Roslin NM, Alvarez N, Giuffre M, et al. Exome sequencing identifies a novel variant in ACTC1 associated with familial atrial septal defect. Can J Cardiol 2014;30:181–7.
[17] Monserrat L, Hermida-Prieto M, Fernandez X, Rodriguez I, Dumont C, Cazon L, et al. Mutation in the alpha-cardiac actin gene associated with apical hypertrophic cardiomyopathy, left ventricular non-compaction, and septal defects. Eur Heart J 2007;28:1953–61.
[18] Tian T, Wang J, Wang H, Sun K, Wang Y, Jia L, et al. A low prevalence of sarcomeric gene variants in a Chinese cohort with left ventricular non-compaction. Heart Vessels 2015;30:258–64.
[19] Bos JM, Will ML, Gersh BJ, Kruisselbrink TM, Ommen SR, Ackerman MJ. Characterization of a phenotype-based genetic test prediction score for unrelated patients with hypertrophic cardiomyopathy. Mayo Clin Proc 2014;89:727–37.
[20] Wessels MW, Herkert JC, Frohn-Mulder IM, Dalinghaus M, van den Wijngaard A, de Krijger RR, et al. Compound heterozygous or homozygous truncating MYBPC3 mutations cause lethal cardiomyopathy with features of noncompaction and septal defects. Eur J Hum Genet 2015;23:922–8.
[21] Andersen PS, Havndrup O, Bundgaard H, Larsen LA, Vuust J, Pedersen AK, et al. Genetic and phenotypic characterization of mutations in myosin-binding protein C (MYBPC3) in 81 families with familial hypertrophic cardiomyopathy: total or partial haploinsufficiency. Eur J Hum Genet 2004;12:673–7.
[22] Elliott PM, Anastasakis A, Borger MA, Borggrefe M, Cecchi F, Charron P. et al., 2014 ESC Guidelines on diagnosis and management of hypertrophic cardiomyopathy: the Task Force for the Diagnosis and Management of Hypertrophic Cardiomyopathy of the European Society of Cardiology (ESC). Eur Heart J 2014;35:2733–79.
[23] Lang RM, Badano LP, Mor-Avi V, Afilalo J, Armstrong A, Ernande L, et al. Recommendations for cardiac chamber quantification by echocardiography in adults: an update from the American Society of Echocardiography and the European Association of Cardiovascular Imaging. J Am Soc Echocardiogr 2015;28. 1–39.e14.
[24] Ha JW, Oh JK, Redfield MM, Ujino K, Seward JB, Tajik AJ. Triphasic mitral inflow velocity with middiastolic filling: clinical implications and associated echocardiographic findings. J Am Soc Echocardiogr 2004;17:428–31.
[25] Nagueh SF, Appleton CP, Gillebert TC, Marino PN, Oh JK, Smiseth OA, et al. Recommendations for the evaluation of left ventricular diastolic function by echocardiography. J Am Soc Echocardiogr 2009;22:107–33.
[26] Behrmann E, Muller M, Penczek PA, Mannherz HG, Manstein DJ, Raunser S. Structure of the rigor actin-tropomyosin-myosin complex. Cell 2012;150:327–38.
[27] Richards S, Aziz N, Bale S, Bick D, Das S, Gastier-Foster J, et al. Standards and guidelines for the interpretation of sequence variants: a joint consensus recommendation of the American College of Medical Genetics and Genomics and the Association for Molecular Pathology. Genet Med 2015;17:405–24.
[28] Jarvik GP, Browning BL. Consideration of cosegregation in the pathogenicity classification of genomic variants. Am J Hum Genet 2016;98:1077–81.
[29] Schlossarek S, Mearini G, Carrier L. Cardiac myosin-binding protein C in hypertrophic cardiomyopathy: mechanisms and therapeutic opportunities. J Mol Cell Cardiol 2011;50:613–20.
[30] Jiang HK, Qiu GR, Li-Ling J, Xin N, Sun KL. Reduced ACTC1 expression might play a role in the onset of congenital heart disease by inducing cardiomyocyte apoptosis. Circ J 2010;74:2410–8.
[31] Bai F, Caster HM, Dawson JF, Kawai M. The immediate effect of HCM causing actin mutants E99K and A230V on actin-Tm-myosin interaction in thin-filament reconstituted myocardium. J Mol Cell Cardiol 2015;79:123–32.
[32] Chow ML, Shaffer JF, Harris SP, Dawson JF. Altered interactions between cardiac myosin binding protein-C and alpha-cardiac actin variants associated with cardiomyopathies. Arch Biochem Biophys 2014;550–551:28–32.
[33] Muller M, Mazur AJ, Behrmann E, Diensthuber RP, Radke MB, Qu Z, et al. Functional characterization of the human alpha-cardiac actin mutations Y166C and M305L involved in hypertrophic cardiomyopathy. Cell Mol Life Sci 2012;69:3457–79.
[34] Glenn NO, McKane M, Kohli V, Wen KK, Rubenstein PA, Bartman T, et al. The W-loop of alpha-cardiac actin is critical for heart function and endocardial cushion morphogenesis in zebrafish. Mol Cell Biol 2012;32:3527–40.
[35] Kim S-A, Son J, Shim C-Y, Choi E-Y, Ha J-W. Long-term outcome of patients with triphasic mitral flow with a mid-diastolic L wave: prognostic role of left atrial volume and N-terminal pro-brain natriuretic peptide. Int J Cardiovasc Imaging 2017;33:1377–84.
[36] Debl K, Djavidani B, Buchner S, Poschenrieder F, Feuerbach S, Riegger G, et al. Triphasic mitral inflow pattern and regional triphasic mitral annulus velocity in hypertrophic cardiomyopathy. J Am Soc Echocardiogr 2008;21(407):e5–6.
[37] Lam CS, Han L, Ha JW, Oh JK, Ling LH. The mitral L wave: a marker of pseudonormal filling and predictor of heart failure in patients with left ventricular hypertrophy. J Am Soc Echocardiogr 2005;18:336–41.
[38] Coppini R, Ho CY, Ashley E, Day S, Ferrantini C, Girolami F, et al. Clinical phenotype and outcome of hypertrophic cardiomyopathy associated with thin-filament gene mutations. J Am Coll Cardiol 2014;64:2589–600.
[39] Ho CY. Genetics and clinical destiny: improving care in hypertrophic cardiomyopathy. Circulation 2010;122:2430–40.
[40] Nannenberg EA, Michels M, Christiaans I, Majoor-Krakauer D, Hoedemaekers YM, van Tintelen JP, et al. Mortality risk of untreated myosin-binding protein C-related hypertrophic cardiomyopathy: insight into the natural history. J Am Coll Cardiol 2011;58:2406–14.